한국정밀공학회지 제 18권 제 5호 (2001년 5월)
Journal of the Korean Society of Precision Engineering, Vol. 18, No. 5, May 2001.

반도체 캡슐화 성형 공정에 있어서 패들 변형 해석

한세진*, 허용정**

Paddle Shift Analysis During Semiconductor Encapsulation

Sejin Han*, Yong Jeong Huh**

ABSTRACT

본 연구에서는 칩 캡슐화 성형 공정 중의 패들 변형을 해석하기 위한 방법론이 연구되었다. 헬레쇼오 근사 모델에 근거한 유한요소법이 칩 캐비티에서의 유동 해석을 위해 사용되었다. 리드 프레임 상의 구멍을 통한 통과 유동해석을 위한 근사모델이 제안되었다. 본 연구에서 제시된 해석모델에 의해 계산된 값과 실험 값은 잘 일치하였다. 유동해석을 통하여 리드프레임과 패들에 의해 경계를 이루고 있는 상, 하 캐비티간의 압력차가 계산되었다. 최종적으로 패들 변형이 압력차 계산 값을 이용하여 계산되게 된다.

Key Words : Semiconductor(반도체), Leadframe(리드프레임), Encapsulation(캡슐화성형), Paddle Shift(패들변형)

1. Introduction

Semiconductor chips are often encapsulated with an epoxy molding compound for protection and optimal use of the chip.(1)

Among problems during encapsulation, paddle shift is one of the most serious problems. Paddle shift is the movement of the paddle due to the pressure difference between the upper and lower cavities, which is shown in Fig. 1.

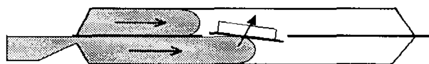

Fig. 1 A schematic of paddle shift during chip encapsulation.

The paddle is where the semiconductor chip sits on. The paddle can move in vertical direction as well as tilt in angle. For accurate paddle-shift analysis, accurate flow analysis is essential. Flow analysis during chip encapsulation is complicated such that computer simulation is often required. Turng and Wang (1993) and Nguyen (1994) have attempted to analyze the flow during encapsulation process numerically.(2)(3)

Particularly, in a study by Turng & Wang (1993), a finite-element method based on the Hele-Shaw approximation is used by assuming the thickness of the chip cavity to be much smaller than its width. The behavior of the fluid(epoxy molding compound) was described by a generalized Newtonian fluid model. On the other hand, although the geometry in the chip cavity is very complicated, analysis was done for a much simplified geometry by treating the leadframe as a solid, neglecting cross flow through the openings in the

* Sibley school of mechanical and Aerospace Engineering, Cornell University
** 한국기술교육대학교 메카트로닉스공학부

leadframe. A connector (which allows unrestricted flow between the two points it connects) was used to connect the flow between the two cavities separated by a leadframe. This treatment is acceptable for rough calculation but for paddle-shift analysis, a more rigorous flow analysis is called for. The paddle shift is determined by the pressure difference in two cavities divided by a leadframe. Because the cross flow in the leadframe will affect the pressure difference significantly, it has to be analyzed rigorously.

In this paper, an effort has been made to analyze the flow in the chip cavity more accurately, so that the paddle-shift calculation can be done accurately. We still use the Hele-Shaw approximation for cavity flow analysis instead of a three-dimensional-flow analysis. This is because the three dimensional analysis would be too costly due to the complicated geometry in the chip cavity (particularly the leadframe). There are typically several hundred openings in the leadframe and it would be almost impossible to model each opening exactly by three dimensional geometry.

After flow analysis, the paddle shift has been calculated using a structural analysis. Elastic material properties and nonlinear geometry have been used in the calculation.

In the next sections, details of the flow analysis and paddle-shift calculation will be presented.

2. Analysis

2.1 Governing Equations for Flow Analysis

The elasticity of the epoxy molding compound is considered negligible if the degree of cure of the sample is low. Because we are only interested in the filling stage of encapsulation where the degree of cure of the sample is low, we will neglect the elasticity of the fluid and thus assume the flow to be generalized Newtonian.[4]

Also, typically the thickness of the chip cavity is much smaller than its width, so the generalized Hele-Shaw approximation can be used.[5] If we make use of these approximations, we can get the following equations for the flow analysis which is similar to that used in the reference (3) and (6). See Fig. 2(a).

Continuity Equation

Including the possible compressibility of the melt, the continuity equation can be written as follows :

$$\frac{\partial \rho}{\partial t} + \frac{\partial(\rho u)}{\partial x} + \frac{\partial(\rho v)}{\partial y} + \frac{\partial(\rho w)}{\partial z} = 0 \qquad (1)$$

Where, ρ is the density, t is the time and u, v, w are the velocity in x, y and z coordinate, respectively (z coordinate represents the thickness direction).

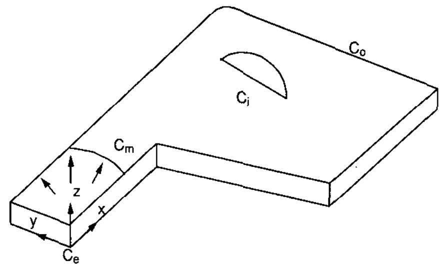

Fig. 2(a) Schematic diagram of flow in a thin cavity. (C_e refers to entrance into cavity, C_m to the advancing melt front, C_i to possible inserts in the mold and C_o to the outer boundary of cavity)

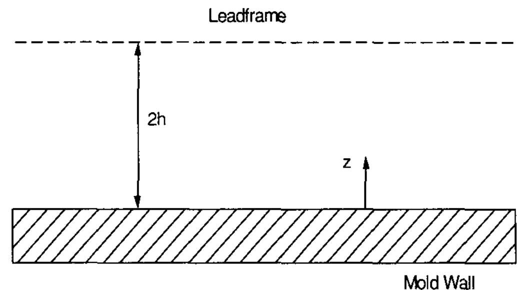

Fig. 2(b) Coordinate in the thickness direction. The cavity is thin in the z direction with a gap thickness of 2h. Here z = 0 corresponds to the mold wall and z = 2h corresponds to the leadframe

Momentum Equation

Neglecting the inertia terms and making use of the thin cavity approximation, the momentum equation in the x and y directions can be written as follows, respectively:

$$\frac{\partial}{\partial z}\left(\eta \frac{\partial u}{\partial z}\right) - \frac{\partial p}{\partial x} = 0 \qquad (2)$$

$$\frac{\partial}{\partial z}(\eta\frac{\partial v}{\partial z}) - \frac{\partial p}{\partial y} = 0 \quad (3)$$

Where, η is the viscosity and p the pressure.

The momentum equation in z direction simply results in constant pressure in z direction.

Energy Equation

Also, by assuming a thin cavity and including heating due to shearing and curing, the energy equation can be written as follows:

$$\rho C_p(\frac{\partial T}{\partial t} + u\frac{\partial T}{\partial x} + v\frac{\partial T}{\partial y} + w\frac{\partial T}{\partial z}) = \frac{\partial}{\partial z}(k\frac{\partial T}{\partial z}) + \eta\gamma^2 + \frac{d\alpha}{dt}H \quad (4)$$

Where, C_p is the heat capacity, T is the temperature, k is thermal conductivity, η viscosity, γ the shear rate, degree of cure and H heat generation due to curing.

Curing Equation

This equation is for the evolution of degree of cure with time. In this study, the empirical equation of Kamal will be used. [7] :

$$(\frac{\partial \alpha}{\partial t} + u\frac{\partial \alpha}{\partial x} + v\frac{\partial \alpha}{\partial y} + w\frac{\partial \alpha}{\partial z}) = (K_1 + K_2\alpha\mu)(1-\alpha)^v$$

$$K_1 = A_1 \exp(-E_1/T)$$

$$K_2 = A_2 \exp(-E_2/T) \quad (5)$$

Where μ , v, A_1, A_2, E_1 and E_2 are fitting constants.

Boundary Conditions

The boundary conditions in the gapwise direction are as follows. The no slip conditions at the wall in the thickness direction will be used for the planar velocity components (u and v). For the velocity component in the thickness direction (w), no slip at the mold wall but a finite cross-flow velocity at the leadframe (W) will be assumed. For temperature, the melt at the mold wall will be assumed to be at the mold wall temperature (T_{W_1}), but the melt at the leadframe will be assumed at temperature (T_{W_2}) which can be different from T_{W_1} (See Fig. 2(b)).

Therefore,

$u = 0, v = 0, w = 0, T = T_{W_1}$ at $z = 0$

$u = 0, v = 0, w = W, T = T_{W_2}(t)$ at $z = 2h$ (6a)

It is convenient to introduce the parameter which is defined by

$$\frac{\partial u}{\partial z} = \frac{\partial v}{\partial z} = 0 \quad \text{at} \quad z = \lambda \quad (6b)$$

The boundary conditions in the planar coordinates are as follows :

At Inlet (C_e):

Pressure : assumed to be uniform but time-dependent.

Temperature : constant at plunger temperature

Degree-of-cure : progresses at plunger temperature

Along the outer boundary of cavity (C_o) and boundary of possible inserts (C_i):

Pressure : $v_n = \frac{\partial p}{\partial n} = 0$ (7)

Temperature or degree-of-cure : No condition

At melt front (C_m):

The pressure is assumed to be zero. Other properties of the sample (temperature, degree of cure) in the melt-front region need special treatment. In this study, we assume that properties at z_2 at the current time step are obtained by the values at z_1 in the previous time step, where z_1 and z_2 are determined from the following equation:

$$\int_0^{z_1}\rho(u-\bar{u})dz + \int_{z_2}^{2h}\rho(u-\bar{u})dz = 0 \quad (8)$$

in which $\bar{u}$ denotes the gapwise-averaged velocity. This equation represents the instantaneous turn-over rule [8].

2.2 Hele-Shaw Formulation

Following the reference (5), (6) and (9), we can calculate the mass flow rate in x, y direction as follows:

$$\int_0^{2h}\rho\, udz = -\tilde{S}\frac{\partial p}{\partial x} \quad (9)$$

$$\int_0^{2h}\rho\, vdz = -\tilde{S}\frac{\partial p}{\partial y} \quad (10)$$

Where, $\tilde{S}$ is calculated by

$$\tilde{S} = \int_0^{2h} \rho \int_0^z \frac{(\lambda - \tilde{z})}{\eta} d\tilde{z}\, dz \tag{11}$$

Then the continuity equation becomes

$$\frac{\partial}{\partial t}\int_0^{2h} \rho dz - \frac{\partial}{\partial x}(\tilde{S}\frac{\partial p}{\partial x}) - \frac{\partial}{\partial y}(\tilde{S}\frac{\partial p}{\partial y}) = -\rho w \tag{12}$$

After calculating p, the velocities can be obtained by

$$u = \frac{\partial p}{\partial x}\int_0^z \frac{(\tilde{z} - \lambda)}{\eta} d\tilde{z} \tag{13}$$

$$v = \frac{\partial p}{\partial y}\int_0^z \frac{(\tilde{z} - \lambda)}{\eta} d\tilde{z} \tag{14}$$

and can be determined by

$$\lambda = \int_0^{2h} \frac{z}{\eta} dz \;/\; \int_0^{2h} \frac{1}{\eta} dz \tag{15}$$

The above equations can be solved by finite-element method as in the reference (3), (5) and (6).

2.3 Flow Through Leadframe Openings

In most cases, the gate is located either upper or lower cavity and cross flow through leadframe opening take place as shown in Fig. 3. We propose a model for the flow through the leadframe openings. This model is for a power-law fluid. Knowing that most epoxy molding compounds have power-law dependence of viscosity on shear rate, this model should be a useful one. The shape of the opening in the leadframe is usually rectangular and the aspect ratio is quite large. Therefore, we can approximate the flow in the opening as a planar flow between parallel plates.

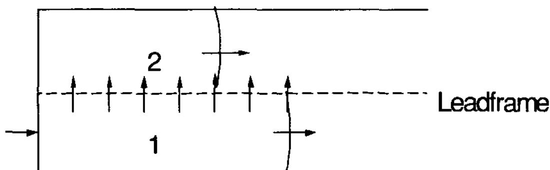

Fig. 3 Schematic diagram of cross flow through the leadframe openings

For a power-law fluid, the shear viscosity and shear rate can be related as follows:

$$\eta = \eta_0(\dot{\gamma})^{n-1} \tag{16}$$

Where n is the power-law index for shear flow and η_0 is a constant.

On the other hand, the extensional viscosity (μ) and the extensional rate ($\dot{\varepsilon}$) are related by:

$$\mu = \mu_0(\dot{\varepsilon})^{m-1} \tag{17}$$

Where, m is the power-law index for extensional flow and μ_0 is a constant.

For the planar flow case, η_0, μ_0, n and m are related as follows.[10]:

$$\mu_0 = 2^{n+1}\eta_0 \tag{18}$$

$$m = n \tag{19}$$

The pressure drop for the flow through the leadframe opening can be calculated as indicated below. The pressure drop consists of the pressure drop in the entrance region (1), in the exit region (2) and in the opening region (3) (See Fig. 4).

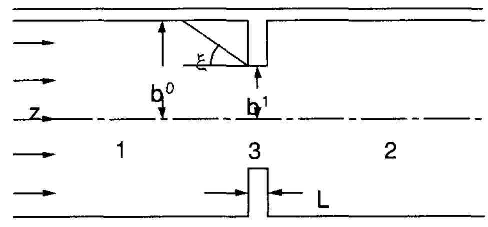

Fig. 4(a) A geometry for the flow through a leadframe opening ($2b_1$ corresponds to leadframe opening size)

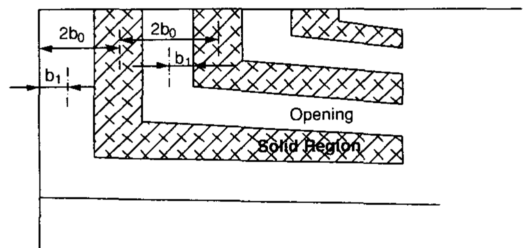

Fig. 4(b) Calculation of b_0 and b_1 for the leadframe

The pressure drop in the entrance or exit region consists of viscous loss, extensional loss and exit loss.[10][11] Each term of the pressure drop in the entrance or exit region can be represented as follows:

$$\Delta P_s = \frac{\eta_0}{2n\xi}\left(\frac{\sin\xi}{\xi}\right)^{2n}\left(\frac{Q}{2}\frac{2n+1}{n}\right)^n\left(\frac{1}{b_0^{2n}}-\frac{1}{b_1^{2n}}\right) \quad (20)$$

$$\Delta P_e = \frac{\mu_0}{2m}\left(\frac{Q}{2}\frac{\sin 2\xi}{\xi}\right)^m\left(\frac{1}{b_0^{2m}}-\frac{1}{b_1^{2m}}\right) \quad (21)$$

$$\Delta P_c = \mu_0\left(\frac{Q}{2b_1^2}\right)^m\int_\xi^0 \frac{\sin^{2m-1}\beta(\beta\cos\beta-\sin\beta)}{\beta^{m+1}}d\beta \quad (22)$$

Where Q is the flow rate through the particular opening (with thickness of $2b_1$) per unit width and b_0 is half of the upstream region thickness, b_1 is half of the opening region thickness. The actual pressure drop in the entrance or exit region corresponds to the value of ξ which minimizes the total entrance or exit pressure drop (the sum of Δp_S (viscous loss), Δp_e (extensional loss) and Δp_c (exit loss)).

The pressure drop in the opening region (region 3 of Fig. 2) can be calculated as the sum of the pressure drop for fully-developed flow and an extra pressure drop in the developing-flow region. The pressure drop for fully-developed flow of a power-law fluid can be written as

$$\Delta P_L = \left[\frac{2(1+2n)Q}{n(2b_1)^2}\right]^n\frac{2\eta_0 L}{2b_1} \quad (23)$$

Where, L is length of the parallel plane (in this case, the thickness of leadframe). The extra pressure drop in the developing-flow region has been determined by simulating the flow in that region using finite element method. The results are as shown in Fig. 3 for creeping flow and a fluid with n = 0.74. The extra pressure loss has been fitted by the following equation.

$$\Delta P_x = 2K_x\eta_0\left[\frac{2(1+2n)Q}{n(2b_1)^2}\right]^n \quad (24)$$

Where,

$K_X = 0$ when $Z < 0.01$

$K_X = A + B\ln(Z)$ when $0.01 < Z < 0.33$

$K_X = C$ when $Z > 0.33$

Where Z is the coordinate in the leadframe opening normalized to b_1 with origin at the starting point of the leadframe (z/b_1). And n=0.74, A = 1.2041, B = 0.2501 and C=0.903. The values of A, B and C only slightly depend on n, so these values can be used for other values of n. For approximation, ξ can be taken as $\pi/2$. Then, the integral term in equation (22) can be approximated by :

$$\int_\xi^0 \frac{\sin^{2n-1}\beta(\beta\cos\beta-\sin\beta)}{\beta^{n+1}}d\beta \tilde{=} an^2-bn+c \quad (25)$$

Where a is 0.04324, b is 0.2042 and c is 0.4504.

Therefore, the total pressure drop between the two cavities is

$$p_t = 2(p_S + p_e + p_c) + p_L + p_X \quad (26)$$

The factor 2 in the above equation appears because the related pressure drop occurs in the entrance and exit regions. These equations can be used to account for the pressure drop during flow through the leadframe openings. Actual implementation can be done in the following two ways.

In this approach, we can connect lower and upper cavities of chip using cross-flow elements. This cross-flow element is to account for the cross flow through the openings. In this case, W = 0 in equation (12). We can use equations (20) - (26) to find the thickness of cross-flow element by making pressure drop across this element the same as that obtained from equation (26). The half-thickness of the cross-flow elements to be used in the modeling can be calculated by the following equations which is derived from equations (20) - (26).

$$b_1^* = A^{-(1/(2n+1))} \quad (27)$$

Where,

$$A = \left(\frac{2n}{1+2n}\right)^n\frac{1}{L}\left\{2\left(\frac{2n+1}{2n}\right)^n\frac{1}{n\xi}\left(\frac{\sin\xi}{\xi}\right)^{2n}\left(\frac{1}{b_0^{2n}}-\frac{1}{b_1^{2n}}\right)\right.$$
$$+\frac{1}{n}\left(\frac{\sin^2\xi}{\xi}\right)^n\left(\frac{1}{b_0^{2n}}-\frac{1}{b_1^{2n}}\right)+\frac{8}{b_1^{2n}}\int_\xi^0\frac{\sin^{2n-1}\beta(\cos\beta-\sin\beta)}{\beta^{n+1}}d\beta$$
$$\left.+\left(\frac{1+2n}{2n}\right)^n\frac{L}{b_1^{2n+1}}+2\left(\frac{1+2n}{2n}\right)^n\frac{K_x}{b_1^{2n}}\right\} \quad (28)$$

On the other hand, the length of the cross-flow

element is the same as the thickness of the leadframe and its width is the same as that of the opening.

In some regions there are too many openings to be modeled one by one in the simulation (for example, there are tens of openings in the chip side region). The following equation can be used to combine N openings of the same thickness into one with its thickness determined from the following equation:

$$b_1^{**} = N^{1/(2n+1)} b_1^{*} \quad (29)$$

2.4 Cavity Thickness and Shape Factor

On the other hand, the thickness of the upper and lower cavities are determined as in Fig. 5.

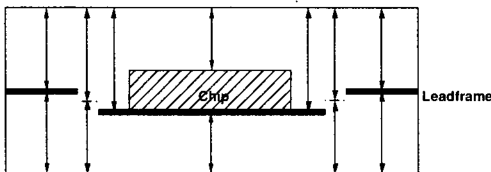

Fig. 5 Modeling of thickness in the chip cavity (arrows represent the cavity thickness to be used in the simulation at each region)

In essence, thickness of each region is the thickness of the cavity separated by the leadframe. The openings of the leadframe will also affect the planar flow in the cavity as well as the cross flow. The flow through cavity with openings will have less resistance than that in a cavity without any opening. To account for this, the "shape factor" concept has been used. The shape factor can be determined from the following equation:

$$\text{Shape factor} = A_{ac} / A_s \quad (30)$$

Where

A_{ac} = Actual area of solid wall in the thickness direction.

A_s = Area of solid wall in the simulation in the thickness direction.

The pressure drop in a region with a shape factor of "s" will have pressure drop of "s" times the pressure drop in the same region but with a shape factor of 1. The shape factors of the side and periphery region for the current case are thus determined to be 0.8 and 0.5, respectively.

2.5 Paddle-Deformation Analysis

During the encapsulation of IC chips, pressure in the upper and lower cavity can be different. This causes the paddle to deform from its original location. As the thickness of the package decreases, even a small displacement of the paddle causes severe problems in reliability of the package.

If the leadframe deforms, the cavity thickness for the flow also changes. This will in turn change the pressure distribution. Therefore, iteration between flow analysis and leadframe deformation analysis must be done for each step of encapsulation process.

In this study, the flow simulation has been done using the C-MOLD Reactive Molding program. The results from this simulation will give the pressure difference between the upper and lower cavities. This pressure difference information will be used to calculate the leadframe deformation. ABAQUS was used for this purpose. Nonlinear analysis must be used because of the large deformation. Also because of the high viscosity of the EMC, we neglect the elastic springback of the leadframe after loading on the leadframe is removed. Also, possible pressure difference during the packing stage is neglected.

3. Example

An example is used for a sample paddle-shift calculation. Fig. 6(a) shows the mold cavity configuration. The chip cavity dimensions are 20 x 20 x 1.4 mm. The fill time is 3.4 seconds, the mold temperature is 175 ^{o}C, and the initial pellet temperature is 90 ^{o}C.

The leadframe used in the deformation analysis consists of a paddle and four legs of leadframe. In the deformation calculation, the 4 ends of leadframe legs have been assumed to be clamped (that is, no translation and no rotation at those points). The leadframe material has 1.21×10^{11} Pa of elastic modulus and the leadframe has 0.125 mm of thickness. The paddle is 12 mm long. The chip cavity size is 20 (length) x 20 (width) x 1.4 mm (thickness).

For the analysis, some material properties were measured. These include viscosity, curing kinetics, thermal conductivity and heat capacity.

The viscosity has been measured from a slit rheometer.[12] Measurement has been done at different temperature, shear rate and degree of cure. The measured viscosity is fitted using the following extended Macosko's model.[13]

$$\eta(\alpha,T,\dot{\gamma}) = \frac{\eta_0(T)}{1+\left(\frac{\eta_0(T)\dot{\gamma}}{\tau^*}\right)^{1-n}}\left(\frac{\alpha_g}{\alpha_g-\alpha}\right)^{(C_1+C_2\alpha)} \quad (31)$$

$$\eta_0(T) = B\exp(T_b/T) \quad (32)$$

Where n, τ^*, B, T_b, C_1, C_2, and α_g are constants. Equation (31) is equivalent to equation (16) if τ^* is small enough.

The curing kinetics were measured using differential scanning calorimetry (DSC). Non-isothermal scannings were performed at three different rates (5, 10 and 20 ^oC/min). The results are fitted using the Kamal's model (equation 5).

Besides these, thermal conductivity and heat capacity have been measured and are as shown in Table 1. Heat capacity is represented as piecewise linear in temperature and thermal conductivity is assumed to be constant.

Table 1 Parameters for the viscosity, curing kinetics and other properties of an epoxy molding compound from Sumitomo

N	0.7764	Temp.(°C)	Heat capacity (J/kg-K)
τ^*(Pa)	1e-4	60	964.3
B(Pa*s)	5.187e-4	100	1061
T_b(K)	6531.0	150	1206
C_1	0.1548	190	1256
C_2	1.057		
α_g	0.4179		
μ	0.5373		
ν	1.258		
A_1 (1/s)	2.34e8		
A_2 (1/s)	4.978e6		
E_1 (K)	1.073e4		
E_2 (K)	8.206e3		
Thermal conductivity (W/m-K)			0.79

Flow analysis has been performed by modeling cross flow as in section 2. For the leadframe used in the current study, openings in the leadframe exist at the corner, side and periphery of the chip. The thickness of cross-flow elements has been determined using equation (30). For example, for the cross-flow elements at the periphery, b_0 = 0.85 mm and b_1 = 0.425 mm which gives b_1^* = 0.25 mm.

It is noted that the effect of wire has been neglected in the simulation because of the small size of wire. As for the temperature, the leadframe was assumed to be at the mold temperature because of the high thermal conductivity of leadframe.

The finite-element mesh generated for the analysis is shown in Figure 6(b).

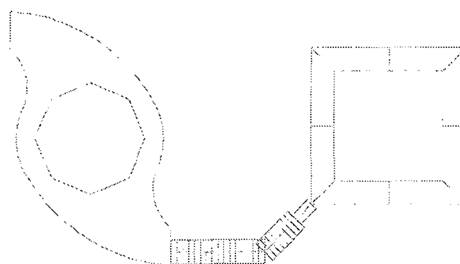

Fig. 6(a) Geometry of the chip cavity used in the encapsulation

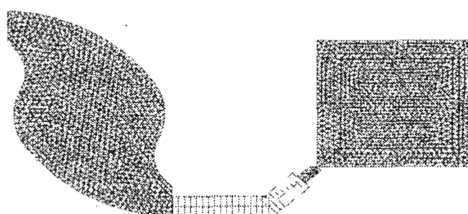

Fig. 6(b) Finite-element mesh of the chip cavity used in the simulation

Some of the calculation results are shown in Fig. 7-11. Fig. 7(a) shows the pressure calculated at the end of filling. The maximum pressure is about 0.17 Mpa. Fig. 7(b) shows the temperature calculated at the end of filling. The temperature distribution is about 60^oC at the pot, and is close to 175^oC at the cavity. Fig. 7(c) shows the bulk degree of cure at the end of filling. The bulk

degree of cure varies from 0% to 3% inside the cavity.

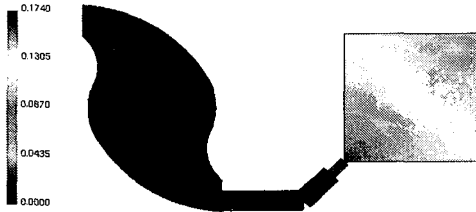

Fig. 7(a) Pressure (Mpa) at the end of filling

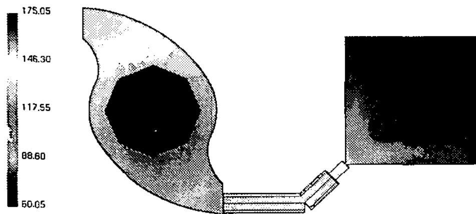

Fig. 7(b) Bulk temperature at the end of filling

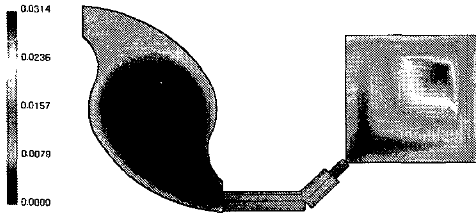

Fig. 7(c) Bulk degree of cure at the end of filling

From the calculated pressure, pressure difference across the leadframe has been calculated as in Fig. 8.

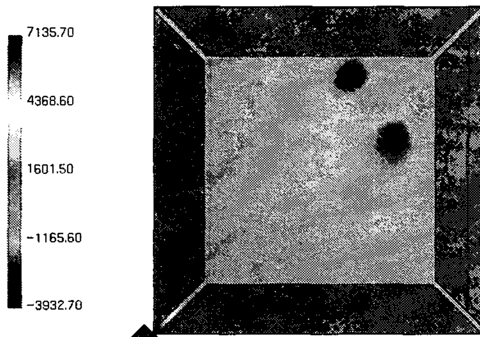

Fig. 8 Maximum pressure difference calculated at the chip cavity

The maximum pressure difference is about 7000 Pa which is much lower than the absolute pressure value. This pressure difference will be applied as a loading to the leadframe for the paddle-deformation. Elastic material properties together with nonlinear geometry were used in the calculation.

The calculated paddle shift values are shown in Fig. 9. As shown in this Figure, the maximum paddle-shift value is about 0.03mm. The stress values calculated are shown in Fig. 10. The maximum stress is on the order of 1 Mpa. This is much lower than the elastic limit of the leadframe. This indicates that the leadframe deformation will be elastic. The calculated strain values are also shown in Fig. 11. As can be seen from this figure, the strain is very small (on the order of 10^{-5}).

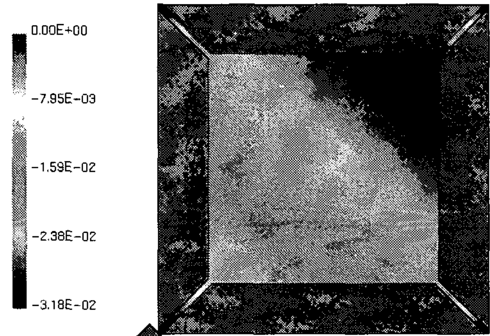

Fig. 9 Calculated displacement of the paddle in z direction that corresponds to the maximum pressure difference

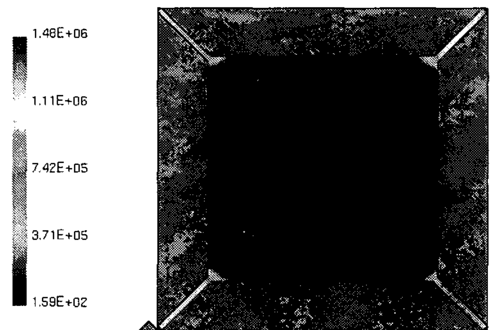

Fig. 10(a) Axial stress calculated that corresponds to the maximum pressure difference

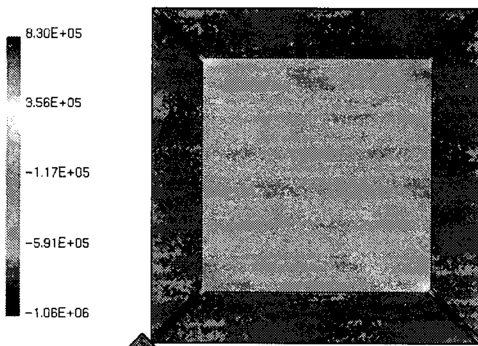

Fig. 10(b) Shear stress calculated that corresponds to the maximum pressure difference

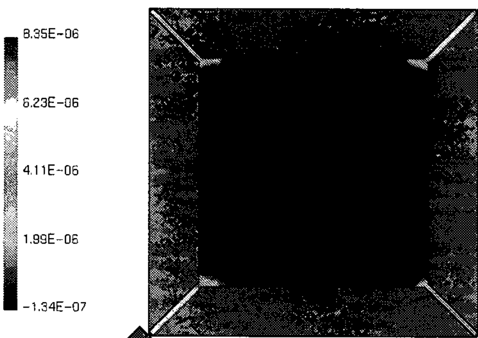

Fig. 11(a) Calculated axial strain that corresponds to the maximum pressure difference

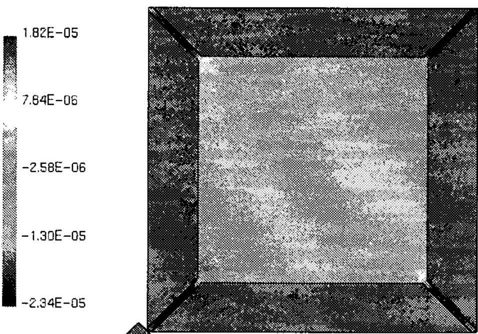

Fig. 11(b) Calculated shear strain that corresponds to the maximum pressure difference

4. Conclusion

Methods to analyze the paddle during semiconductor chip encapsulation have been successfully developed. A finite element method based on Hele-Shaw approximati on is used for the flow analysis in chip cavity. Also, approximate models for the cross flow through the leadframe openings have been made.

From the flow analysis, pressure difference across the leadframe and paddle has been calculated.

The paddle shift was calculated from the pressure difference information.

References

1. Manzione, L. T., "Plastic Packaging of Microelectronic Devices," Van Nostrand Reinhold, New York, 1990.
2. Nguyen, "Flow simulation in IC chip encapsulation," ECTC Conference, Buena Vista, FL, 1994.
3. Turng, L. S. and V. W. Wang, "On the Simulation of Microelectronic Encapsulation with Epoxy Molding Compound," *Journal of Reinforced Plastics and Composites*, Vol. 12, pp. 506-519, 1993.
4. Bird, R. B., Armstrong, R. C. and Hassager, O., "Dynamics of Polymeric Liquids," Vol. 1, Wiley-Interscience, New York, 1987.
5. Hieber, C. A. and Shen, S. F., 1980, "A Finite-Element/Finite-Difference Simulation of the Injection-Molding Filling Process," *J. Non-Newtonian Fluid Mechanics*, Vol. 7, pp. 1-32, 1980.
6. Chiang, H. H., Hieber, C. A. and Wang, K. K., "A Unified Simulation of the Filling and Postfilling Stages in Injection Molding," Part I and II, *Polym. Eng. Sci.*, Vol. 31, pp. 116-139, 1991.
7. Kamal, M. R. and Ryan, M. E., Chapter 4 of "Injection and Compression Molding Fundamentals," A. I. Isayev(editor), Marcel Dekker, New York, 1987.
8. Gonzalez, U. F, Ph.D. Thesis, Cornell University, Ithaca, NY., 1991.
9. Tucker, C. L., Chapter 7 of "Injection and Compression Molding Fundamentals," A. I. Isayev (editor), Marcel Dekker, New York, 1987.
10. Gupta, M., "Juncture loss in an entrance region for polymeric materials," SPE Technical Papers, 1995.
11. Gibson, A. G., Chapter 3 of "Rheological Measurement," Collyer, A. A. and Clegg, D. W. (editor), Elsevier Applied Science, New York, 1988.

12. Han, S., Wang, K. K., Hieber, C. A. and Cohen, C., "Characterization of the Rheological Properties of a Fast-Curing Epoxy Molding Compound," *J. Rheology*, Vol. 42, pp. 177-195, 1997.
13. Castro, J. M. and Macosko, C. W., "Kinetics and Rheology of Typical Polyurethane Reaction Injection Molding Systems," *SPE Technical Papers*, pp. 434, 1980.